## ANNALS OF "DUNAREA DE JOS" UNIVERSITY OF GALATI MATHEMATICS, PHYSICS, THEORETICAL MECHANICS FASCICLE II, YEAR XVII (XLVIII) 2025, No. 1

DOI: https://doi.org/10.35219/ann-ugal-math-phys-mec.2025.1.02

# Signal analysis based on recurrence plots for effective driver behavior detection

Danut-Dragos Damian<sup>1</sup>, Simona Moldovanu<sup>1,2</sup>, Felicia-Anisoara Damian<sup>3</sup>, Michael Fratita<sup>4</sup>, Luminita Moraru<sup>1,5\*</sup>

#### **Abstract**

This paper employs recurrence plots (RPs) generated from both accelerometer and gyroscope data to analyze driver behavior. It integrates visualization with quantitative analysis by extracting key recurrence quantification measures, such as the Recurrence Rate (RR), Determinism (DET), and Laminarity (LAM), to effectively characterize the dynamics of the time-series signals. The accelerometer and gyroscope data are collected along three axes. These recurrence-based features facilitate the discrimination between stable, controlled driving dynamics and irregular, non-deterministic driving behavior. The RPs are generated using a sliding time window. The epoch length is set to 3000 samples with a window overlap of 80%. The results demonstrate that changes in driving conditions significantly altered the structure of the recurrence plots, with corresponding variations in the recurrence quantification RR, DET, and LAM metrics highlighting the sensitivity of these parameters to behavioral dynamics.

**Keywords:** Accelerometer, Gyroscope, Sliding Window, Recurrence Plots, Recurrence Matrix Recurrence Quantification Analysis, Recurrence Rate (RR), Determinism (DET), Laminarity (LAM).

### 1. INTRODUCTION

A responsible driving style, along with advanced safety technologies and adherence to traffic laws, is essential for reducing accidents and saving lives. Ongoing driver education and adapting infrastructure to new challenges are crucial steps toward achieving global and European road safety objectives.

Recent research confirms that the number of vehicles worldwide is steadily increasing. According to a recent analysis by Goldman Sachs, the global vehicle fleet is projected to exceed 2 billion by 2040 (Reuters, 2024) [1]. This trend significantly heightens road safety concerns, particularly as road traffic accidents continue to be a leading cause of death globally, with over 1.19 million fatalities annually. Approximately 12% of these incidents are attributed to driver distraction (World Health Organization, 2023) [2].

<sup>&</sup>lt;sup>1.</sup>The Modelling & Simulation Laboratory, Dunarea de Jos University of Galati, 47 Domneasca Street, 800008 Galati, Romania

<sup>&</sup>lt;sup>2</sup>Department of Computer Science and Information Technology, Faculty of Automation, Computers, Electrical Engineering and Electronics, Dunarea de Jos University of Galati, 47 Domneasca Street, 800008 Galati, Romania

<sup>&</sup>lt;sup>3</sup> Emil Racovita High School of Galati, 12-14, Regiment 11 Siret Street, 800332, Galati, Romania <sup>4</sup> Department of Thermal Systems and Automotives, Faculty of Engineering, Dunărea de Jos University of Galați, 800008 Galați, Romania

<sup>&</sup>lt;sup>5</sup> Department of Physics, School of Science and Technology, Sefako Makgatho Health Sciences University, Pretoria, South Africa

<sup>\*</sup> Corresponding author: luminita.moraru@ugal.ro

In this context, advanced methods for analyzing complex time series, such as Recurrence Plots (RPs) and Recurrence Quantification Analysis (RQA), have shown promise in assessing driving behavior. RPs enable visualization of recurring patterns in system dynamics, while RQA provides quantitative indicators, such as Recurrence Rate (RR), Determinism (DET), and Laminarity (LAM), that describe the stability or unpredictability of driver actions.

In the present study, data collected from accelerometers and gyroscopes, analyzed through sliding windows, reveal that changes in RR, DET, and LAM are sensitive to variations in driver behavior. These findings offer a strong foundation for developing intelligent systems to monitor road safety in real time.

Spiegel [3] introduced a novel method for measuring distances between time series using RPs and RQA. This approach aims to identify representative prototypes encompassing a broad range of recurring driving behavior patterns, regardless of sequence. Experiments using real-world Volkswagen test-drive data demonstrate that this clustering technique identifies recurring patterns more effectively than Dynamic Time Warping (DTW).

Shahverdy et al. [4] proposed a driver behavior classification method that relies solely on vehicle signals, such as acceleration, gravity, pedal pressure, speed, and RPM, without visual input. These signals are transformed into images using the RP technique, and driving behaviors (normal, aggressive, distracted, drowsy, and drunk) are classified using a Convolutional Neural Network (CNN). By exploiting spatial dependencies in the recurrence images, the system achieves high efficiency and low computational cost. Experimental results confirm the system's capability to issue timely alerts to drivers, law enforcement, or nearby vehicles in hazardous situations.

Ashqar et al. [5] focused on detecting so-called "Vulnerable Road Users" (VRUs) using only low-power smartphone sensors. RQA features were extracted from accelerometers, gyroscopes, and rotation vectors, avoiding the high energy consumption of GPS. Combined with traditional time-domain features, RQA features were evaluated using Random Forest classifiers for binary, four-class, and five-class classification tasks. The method achieved 98.34% accuracy using only RQA features and 98.79% when temporal features were included, outperforming previously reported approaches.

Vlahogianni et al. [6] examined the applicability of RPs and RQA in short-term traffic flow analysis through three case studies involving univariate and multivariate data. Their results showed that traffic flow exhibited discontinuous evolution, necessitating robust, pattern-based predictive models over purely continuous data approaches. The study also found that linking statistical characteristics of flow with traffic states can enhance forecast accuracy, advocating for multiple simple models tailored to specific traffic conditions.

RPs and RQA have proven effective in identifying nonlinear and nonstationary patterns in traffic data, contributing to more accurate predictions and improved model selection.

## 2. METHOD

# 2.1. Database and General Study Presentation

The dataset used in this study was published on the Mendeley Data platform by Shardul Nazirkar [7]. It comprises 14,250 dynamic measurements and provides a controlled environment for applying the proposed method based on RPs and RQA. The primary objective is to highlight dynamic distinctions between normal and aggressive driving behaviors.

The algorithm employed in this study is illustrated in Fig. 1.

# Fig. 1. Algorithm for RQA features extraction

**Input:** Accelerometer and gyroscope data (signals on the X, Y, Z axes)

**Output:** Recurrence Rate (RR), Determinism (DET), and Laminarity (LAM) indicators **Steps**:

- 1. {Step 1} Import accelerometer and gyroscope data;
- 2. {Step 2} Apply a sliding time window of 3000 samples with 80% overlap for signal segmentation;
- 3. {Step 3} Generate Recurrence Plots (RP) for each data segment;
- 4. {Step 4} Perform visual analysis of the RPs to identify behavioral patterns (diagonal lines, scattered points, vertical/horizontal structures);
- 5. {Step 5} Extract quantitative RQA features: Recurrence Rate (RR), Determinism (DET), and Laminarity (LAM) from each RP;
- 6. {Step 6} Record the feature values for each time window;
- 7. {Step 7} Repeat steps 1–6 for all available data in the experimental set.

Figure 2 summarizes the flowchart of the proposed method.

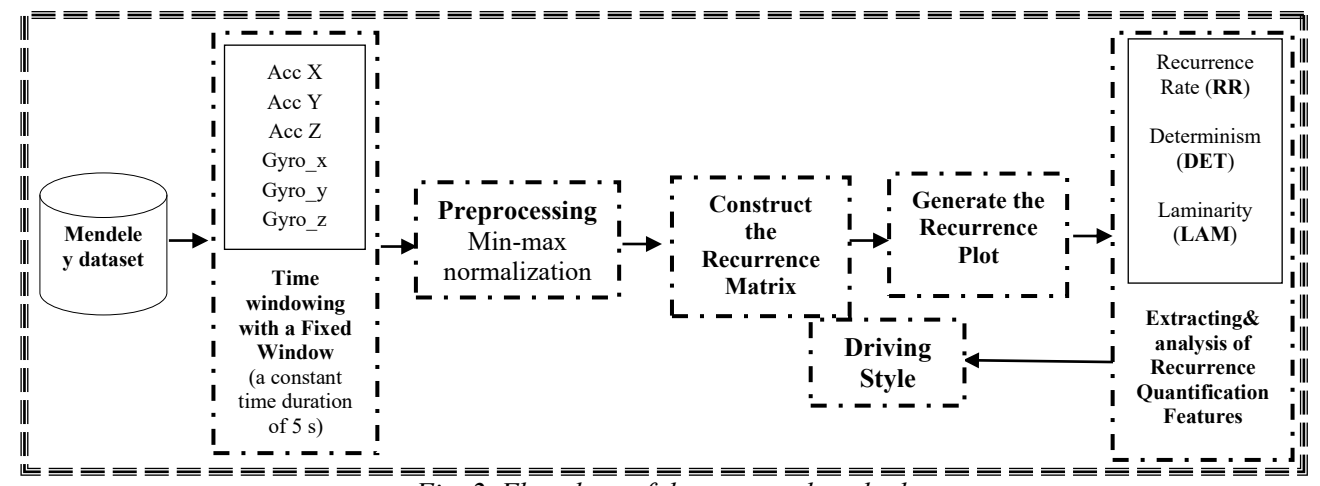


Fig. 2. Flowchart of the proposed method

## 2.2. Mathematical approaches

a) Recurrence Rate (RR) measures the density of recurrence points within a RP [8]:

$$RR = \frac{1}{N^2} \sum_{i,j} R_{ij}$$
 (1)

where  $R_{ii}$  represents the elements of the recurrence matrix and N is the size of the matrix.

b) **Determinism (DET)** quantifies the proportion of recurrence points that form diagonal lines in a Recurrence Plot, indicating the predictability of the system [8]:

$$DET = \frac{\sum_{l=l_{min}}^{N} lP(l)}{\sum_{l=1}^{N} lP(l)}$$
(2)

Where  $l_{min}$  is the minimum diagonal line length (often set to 2 to ignore very short recurrences),

N is the maximum diagonal line length and P(l) is the probability distribution of diagonal line lengths. P(l) represents the probability distribution of diagonal line lengths l in the recurrence plot. It tells us how frequently diagonal lines of a certain length appear.

c) Laminarity (LAM) measures the proportion of recurrence points forming vertical lines within a Recurrence Plot, helping to detect laminar phases such as stop-and-go behavior [8]:

$$LAM = \frac{\sum_{v=v_{min}}^{N} vP(v)}{\sum_{v=1}^{N} vP(v)}$$
(3)

Where P(v) is the probability distribution of vertical line lengths v, and  $v_{min}$  is the minimum vertical line length considered.

The analysis of Recurrence Plots (RPs) is based on the following findings: i) consistent diagonal lines are indicative of periodic and predictable behavior patterns; ii) scattered points suggest random behavior or the occurrence of unexpected events; iii) vertical structures typically correspond to abrupt behavioral changes, such as sudden braking or rapid acceleration [9, 10].

The RQA features are interpreted as follows: i) high DET values (ranging from 0.987 to 0.996) signify predictable and stable driving behavior [9]; ii) elevated LAM values (0.996 to 0.998) indicate controlled motion, reflecting the absence of abrupt trajectory changes [11]; iii) moderate RR values (between 0.63 and 0.83) represent a reasonable degree of repetitiveness, with slight variability likely due to changing traffic conditions [12].

## 3. RESULTS AND DISCUSSION

The objective of this study is to evaluate the stability of driving behavior using RQA metrics computed from accelerometer and gyroscope data over multiple time windows. The signals from the accelerometer (Ox, Oy, Oz) and gyroscope (Gx, Gy, Gz) are labelled in **class 0 (normal behavior)** and **class 1 (aggressive behavior)**.

Figure 3 presents some examples of RPs generated based on the accelerometer and gyroscope data corresponding to the 2, 8 and 18 time windows.

Table 1, 2 and 3 display data obtained for 19 sliding time-windows (5-minute time intervals with a 1-minute time window).

In Table 1, DET values generally ranged between 0.89 and 0.99, with the highest values gathered on the ACC\_X\_0 and GYRO\_X\_0 channels. Time windows 1, 5, and 13 indicated the most predictable and stable driving behavior. Conversely, in windows 16–19, DET showed a moderate decrease across all channels, suggesting slight behavioral instability.

In Table 2, LAM values remained consistently high throughout the recording period, ranging from 0.92 to 0.99. These consistently higher values indicate a frequent presence of stop-and-go behaviors. Among all channels, ACC\_X\_0 and GYRO\_X\_0 exhibited the most stability in LAM values, particularly during the middle time windows. High LAM values persisted even in the final windows, suggesting that driving behavior remained controlled despite more variable traffic conditions.

In contrast, Table 3 shows that RR values exhibited greater variability compared to DET and LAM, fluctuating between 0.63 and 0.86. The highest RR values occurred in windows 5 and 13 (RR > 0.83), especially on the ACC\_X\_0 channel, indicating a strong recurrence of system states. Conversely, a significant decline in RR was observed during windows 16–19, most prominently on the GYRO\_Y\_0 channel, which may reflect a decrease in driving regularity and an increase in behavioral variability.

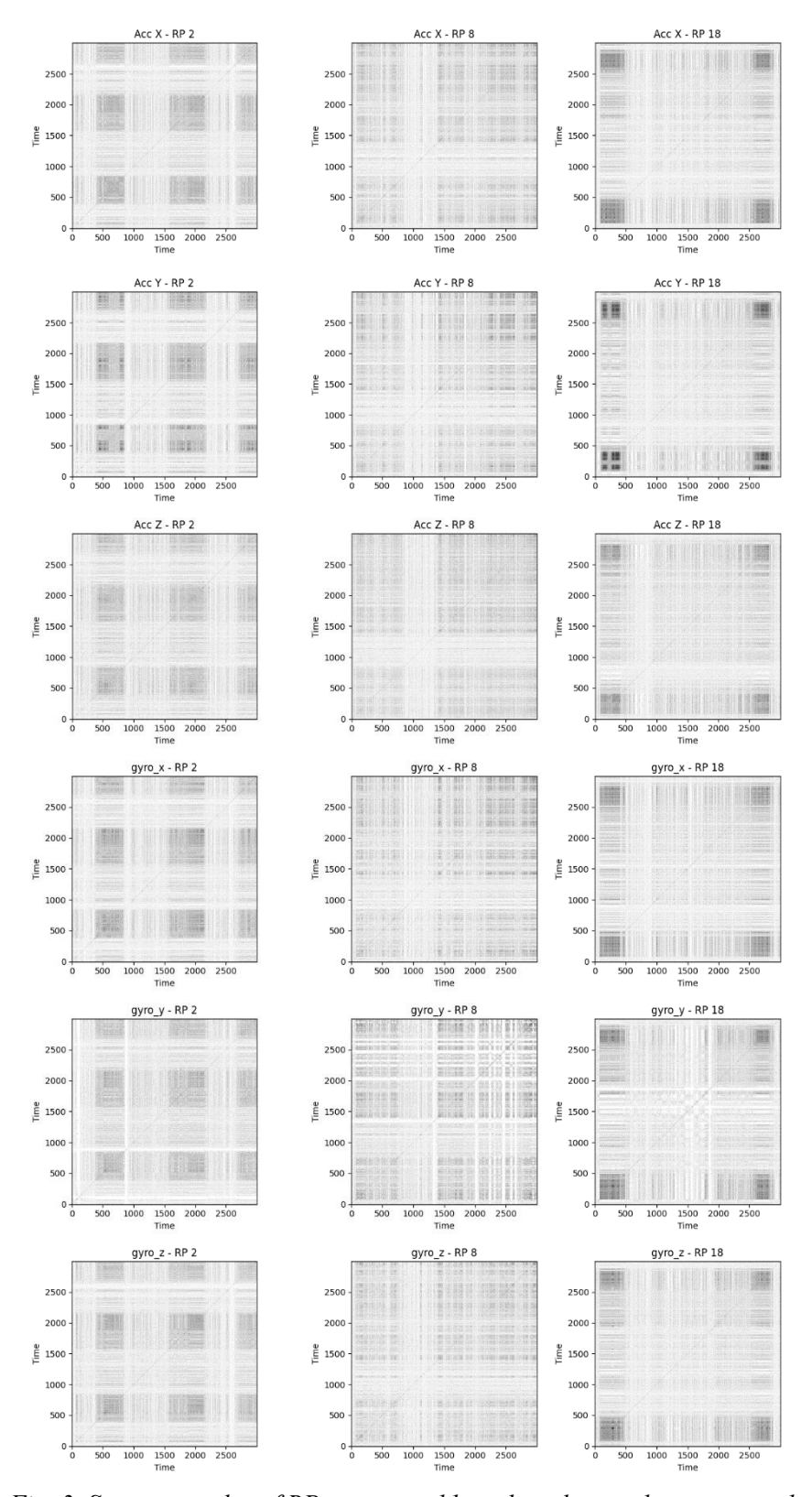


Fig. 3. Some examples of RPs generated based on the accelerometer and gyroscope data corresponding to the 2, 8, and 18 time windows

# Table 1. DET values for each data channel (ACC\_X, ACC\_Y, ACC\_Z, GYRO\_X, GYRO\_Y, GYRO\_Z)

Window	DET ACC-X_0	DET ACC_Y_0	DET ACC_Z_0	DET GYRO_X_0	DET GYRO_Y_0	DET ACC_Z_0	DET ACC_X_1	DET ACC_Y_1	DET ACC_Z_1	DET GYRO_X_1	DET GYRO_Y_1	DET GYRO_Z_1
1	0.98	0.892	0.932	0.947	0.959	0.963	0.987	0.892	0.932	0.947	0.959	0.963
2	0.98	0.914	0.908	0.947	0.969	0.968	0.989	0.914	0.908	0.947	0.969	0.968
3	0.99	0.927	0.919	0.955	0.966	0.972	0.990	0.927	0.919	0.955	0.966	0.972
4	0.98	0.907	0.892	0.936	0.908	0.933	0.988	0.907	0.892	0.936	0.908	0.933
5	0.99	0.950	0.948	0.946	0.932	0.931	0.994	0.950	0.948	0.946	0.932	0.931
6	0.99	0.938	0.938	0.931	0.925	0.927	0.993	0.938	0.938	0.931	0.925	0.927
7	0.99	0.932	0.942	0.928	0.915	0.925	0.992	0.932	0.942	0.928	0.915	0.925
8	0.99	0.936	0.941	0.931	0.930	0.924	0.992	0.936	0.941	0.931	0.930	0.924
9	0.99	0.946	0.954	0.942	0.940	0.937	0.994	0.946	0.954	0.942	0.940	0.937
10	0.98	0.904	0.951	0.928	0.958	0.939	0.989	0.904	0.951	0.928	0.958	0.939
11	0.99	0.933	0.909	0.953	0.964	0.936	0.994	0.933	0.909	0.953	0.964	0.936
12	0.99	0.959	0.943	0.974	0.975	0.969	0.995	0.959	0.943	0.974	0.975	0.969
13	0.99	0.982	0.965	0.978	0.961	0.951	0.995	0.982	0.965	0.978	0.961	0.951
14	0.99	0.978	0.958	0.973	0.953	0.942	0.994	0.978	0.958	0.973	0.953	0.942
15	0.99	0.964	0.940	0.964	0.934	0.920	0.993	0.964	0.940	0.964	0.934	0.920
16	0.98	0.958	0.930	0.956	0.888	0.889	0.987	0.958	0.930	0.956	0.888	0.889
17	0.98	0.969	0.919	0.978	0.892	0.861	0.980	0.969	0.919	0.978	0.892	0.861
18	0.98	0.970	0.925	0.981	0.909	0.878	0.983	0.970	0.925	0.981	0.909	0.878
19	0.98	0.964	0.962	0.977	0.892	0.867	0.983	0.964	0.962	0.977	0.892	0.867

Table 2. Presents the Laminarity (LAM) values for each data channel (ACC\_X, ACC\_Y, ACC\_Z, GYRO\_X, GYRO\_Y, GYRO\_Z)

Window	LAM ACC_X_0	LAM ACC_Y_0	LAM ACC_Z_0	LAM GYRO_X_0	LAM GYRO_Y_0	LAM ACC_Z_0	LAM ACC_X_1	LAM ACC_Y_1	LAM ACC_Z_1	LAM GYRO_X_1	LAMT GYRO_Y_1	LAM GYRO_Z_1
1	0.99	0.926	0.949	0.960	0.967	0.970	0.997	0.926	0.949	0.960	0.967	0.970
2	0.99	0.940	0.933	0.959	0.975	0.975	0.997	0.940	0.933	0.959	0.975	0.975
3	0.99	0.948	0.940	0.965	0.973	0.977	0.997	0.948	0.940	0.965	0.973	0.977
4	0.99	0.933	0.920	0.950	0.929	0.946	0.997	0.933	0.920	0.950	0.929	0.946
5	0.99	0.963	0.961	0.960	0.950	0.946	0.998	0.963	0.961	0.960	0.950	0.946
6	0.99	0.954	0.952	0.948	0.945	0.944	0.998	0.954	0.952	0.948	0.945	0.944
7	0.99	0.948	0.954	0.944	0.938	0.941	0.998	0.948	0.954	0.944	0.938	0.941
8	0.99	0.951	0.953	0.945	0.949	0.941	0.998	0.951	0.953	0.945	0.949	0.941
9	0.99	0.960	0.963	0.956	0.957	0.952	0.998	0.960	0.963	0.956	0.957	0.952
10	0.99	0.928	0.960	0.945	0.968	0.952	0.997	0.928	0.960	0.945	0.968	0.952
11	0.99	0.951	0.930	0.965	0.973	0.950	0.998	0.951	0.930	0.965	0.973	0.950
12	0.99	0.970	0.955	0.980	0.981	0.975	0.998	0.970	0.955	0.980	0.981	0.975
13	0.99	0.987	0.976	0.985	0.973	0.965	0.998	0.987	0.976	0.985	0.973	0.965
14	0.99	0.984	0.972	0.981	0.968	0.959	0.998	0.984	0.972	0.981	0.968	0.959
15	0.99	0.974	0.959	0.975	0.956	0.946	0.998	0.974	0.959	0.975	0.956	0.946
16	0.99	0.968	0.950	0.967	0.924	0.921	0.997	0.968	0.950	0.967	0.924	0.921
17	0.99	0.973	0.939	0.981	0.924	0.895	0.995	0.973	0.939	0.981	0.924	0.895
18	0.99	0.975	0.943	0.984	0.934	0.907	0.996	0.975	0.943	0.984	0.934	0.907
19	0.99	0.969	0.968	0.980	0.922	0.898	0.996	0.969	0.968	0.980	0.922	0.898

Table 3. Presents the Recurrence Rate (RR) values for each data channel (ACC\_X, ACC\_Y, ACC\_Z, GYRO\_X, GYRO\_Y, GYRO\_Z)

Window	RR ACC-X_0	RR ACC_Y_0	RR ACC_Z_0	RR GYRO_X_0	RR GYRO_Y_0	RR ACC_Z_0	RR ACC_X_1	RR ACC_Y_1	RR ACC_Z_1	RR GYRO_X_1	RR GYRO_Y_1	RR GYRO_Z_1
1	0.71	0.687	0.752	0.796	0.791	0.83	0.719	0.687	0.752	0.79	0.791	0.831
2	0.75	0.728	0.707	0.797	0.830	0.85	0.751	0.728	0.707	0.79	0.830	0.851
3	0.75	0.744	0.723	0.815	0.821	0.86	0.757	0.744	0.723	0.81	0.821	0.863
4	0.73	0.700	0.666	0.758	0.687	0.74	0.732	0.700	0.666	0.75	0.687	0.748
5	0.83	0.803	0.784	0.788	0.743	0.74	0.830	0.803	0.784	0.78	0.743	0.744
6	0.80	0.774	0.752	0.748	0.710	0.74	0.803	0.774	0.752	0.74	0.710	0.741
7	0.79	0.760	0.759	0.738	0.659	0.73	0.797	0.760	0.759	0.73	0.659	0.735
8	0.80	0.771	0.762	0.743	0.674	0.73	0.801	0.771	0.762	0.74	0.674	0.735
9	0.83	0.803	0.796	0.776	0.691	0.76	0.833	0.803	0.796	0.77	0.691	0.769
10	0.76	0.688	0.781	0.748	0.724	0.77	0.764	0.688	0.781	0.74	0.724	0.771
11	0.82	0.747	0.686	0.814	0.754	0.76	0.827	0.747	0.686	0.81	0.754	0.762
12	0.84	0.818	0.765	0.880	0.816	0.84	0.844	0.818	0.765	0.88	0.816	0.847
13	0.81	0.914	0.868	0.892	0.808	0.80	0.819	0.914	0.868	0.89	0.808	0.809
14	0.78	0.897	0.846	0.870	0.796	0.78	0.789	0.897	0.846	0.87	0.796	0.782
15	0.74	0.859	0.800	0.842	0.758	0.73	0.746	0.859	0.800	0.84	0.758	0.738
16	0.68	0.831	0.764	0.809	0.644	0.67	0.682	0.831	0.764	0.80	0.644	0.671
17	0.63	0.857	0.731	0.879	0.644	0.62	0.636	0.857	0.731	0.87	0.644	0.622
18	0.66	0.858	0.737	0.894	0.689	0.65	0.666	0.858	0.737	0.89	0.689	0.651
19	0.68	0.835	0.823	0.880	0.619	0.63	0.687	0.835	0.823	0.88	0.619	0.634

RP graphs were generated from accelerometer and gyroscope signals for each time window to provide a visual representation of the system's dynamic behavior. These 2D plots illustrate how system states recur or evolve by capturing similarities between signal sequences. Consequently, RPs offer an intuitive view of the vehicle's stability, variability, and rhythmic patterns, effectively complementing the quantitative insights derived from RQA.

Variations in the lateral acceleration ACC\_Y and roll motion GYRO\_X data are particularly informative for driving behavior characterization. Events such as lane changes, obstacle avoidance maneuvers, or lateral oscillations due to dense traffic leave distinct signatures in these data. Moreover, accumulated driver fatigue may lead to diminished directional control, reflected in more erratic patterns of lateral acceleration and vehicle tilt. When these signal variations are interpreted alongside trends in DET, LAM, and RR values, a coherent behavioral profile emerges. Overall, driving behaviour remained largely stable and predictable throughout the recording, with minor performance degradations observed in the later stages. These deviations are likely attributable to external influences (e.g., increased traffic complexity) or internal factors (e.g., driver fatigue).

#### 4. CONCLUSIONS

This study demonstrated the effectiveness of RQA, combined with RPs generated using a sliding time window (3000-sample epochs with 80% overlap), for evaluating driving behavior based on accelerometer and gyroscope data. The RQA metrics, RR, DET, and LAM, provided detailed insights into driving dynamics across 19 overlapping time windows. We should note that no indications of aggressive driving behavior (class 1) were observed during the analyzed intervals. All findings consistently reflected predominantly normal driving behavior (class 0), with only minor, expected adaptations to external influences such as traffic congestion. The integrated use of RQA and RPs analysis enabled sensitive, quantitative assessments of driving behavior and offered intuitive visual confirmation of the results. These methods present a robust and scalable approach for continuous driver monitoring and road safety evaluation.

Future research may further strengthen this framework by incorporating predictive algorithms for early signs of driver fatigue or risky behavior detection in real time.

#### References

- 1. Reuters, Road oil demand to peak by 2032 as EVs become more popular, Goldman forecasts, Reuters, (2024). https://www.reuters.com/markets/commodities/road-oil-demand-peak-by-2032-evs-become-more-popular-goldman-forecasts-2024-04-02/
- 2. World Health Organization (WHO), Global Status Report on Road Safety 2023, (2023). https://www.who.int/teams/social-determinants-of-health/safety-and-mobility/global-status-report-on-road-safety-2023
- 3. Spiegel S., Discovery of driving behavior patterns, in: Smart Information Systems: Computational Intelligence for Real-Life Applications, Springer, Cham, (2015) 315–343.
- 4. Shahverdy M., Fathy M., Berangi R., Sabokrou M., Driver behavior detection and classification using deep convolutional neural networks, Expert Systems with Applications 149 (2020) 113240.
- 5. Ashqar H.I., Elhenawy M., Masoud M., Rakotonirainy A., Rakha H.A., Vulnerable Road User Detection Using Smartphone Sensors and Recurrence Quantification Analysis, in: 2019 IEEE Intelligent Transportation Systems Conference (ITSC), IEEE, Auckland, (2019) 1054–1059.
- 6. Vlahogianni E.I., Karlaftis M.G., Golias J.C., Recurrence analysis applications to short-term macroscopic and microscopic road traffic, in: Webber C.L., Marwan N. (Eds.), Recurrence Quantification Analysis, Understanding Complex Systems, Springer, Cham, (2015) 375–397.
- 7. Nazirkar S., Phone sensor data while driving a car and normal or aggressive driving behaviour classification, Mendeley Data, V1 (2021). https://doi.org/10.17632/5stn873wft.1
- 8. Pánis R., Adámek K., Marwan N., Averaged recurrence quantification analysis, The European Physical Journal Special Topics 231(3) (2022) 395–411.
- 9. Marwan N., Romano M.C., Thiel M., Kurths J., Recurrence Plots for the Analysis of Complex Systems, Physics Reports 438 (2007) 237–329.
- 10. Webber C.L., Zbilut J.P., Dynamical Assessment of Physiological Systems and States Using Recurrence Plot Strategies, Journal of Applied Physiology 76(2) (1994) 965–973.
- 11. Eckmann J.P., Kamphorst S.O., Ruelle D., Recurrence Plots of Dynamical Systems, Europhysics Letters 4(9) (1987) 973–977.
- 12. Eroglu D., Marwan N., Prasad S., Schinkel S., Kurths J., Finding recurrence networks' threshold adaptively for a specific time series, Nonlinear Processes in Geophysics 21(6) (2014) 1085–1092.